

NACA RM No. L8H10

7143

RM L8H10

Declassified by Authority of LARC Security Classification
officer (SCO) Letter dated June 16, 1983

Maxine F. Sommer

408

~~RESTRICTED~~

Copy No. 134

RM No. L8H10



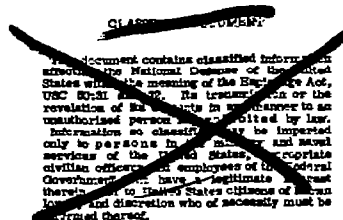
RESEARCH MEMORANDUM

EFFECT OF AIRFOIL PROFILE OF SYMMETRICAL SECTIONS ON THE
LOW-SPEED STATIC-STABILITY AND YAWING DERIVATIVES OF
45° SWEEPBACK WING MODELS OF ASPECT RATIO 2.61

By

William Letko and Byron M. Jaquet

Langley Aeronautical Laboratory
Langley Field, Va.



AFM 28
TECHNICAL 1 Series
AFL 28H

NATIONAL ADVISORY COMMITTEE
FOR AERONAUTICS

WASHINGTON

November 9, 1948

~~RESTRICTED~~

319.98/13

Reply to Attn of

139A

JUN 1 6 1983

TO: Distribution

FROM: 180A/Security Classification Officer

SUBJECT: Authority to Declassify NACA/NASA Documents Dated Prior to
January 1, 1960

(informal, correspondence)
Effective this date, all material classified by this Center prior to
January 1, 1960, is declassified. This action does not include material
derivatively classified at the Center upon instructions from other Agencies.

Immediate re-marking is not required; however, until material is re-marked by
lining through the classification and annotating with the following statement,
it must continue to be protected as if classified:

"Declassified by Authority of LARC Security Classification Officer (SCO)
letter dated June 16, 1983," and the signature of person performing the
re-marking.

If re-marking a large amount of material is desirable, but unduly burdensome,
custodians may follow the instructions contained in NHB 1640.4, subpart F,
section 1203.604, paragraph (h).

This declassification action complements earlier actions by the National
Archives and Records Service (NARS) and by the NASA Security Classification
Officer (SCO). In Declassification Review Program 807008, NARS declassified
the Center's "Research Authorization" files, which contain reports, Research
Authorizations, correspondence, photographs, and other documentation.
Earlier, in a 1971 letter, the NASA SCO declassified all NACA/NASA formal
series documents with the exception of the following reports, which must
remain classified:

Document No.

First Author

E-51A30
E-53G20
E-53G21
E-53K18
SL-54J21a
E-55C16
E-56H23a

Nagey
Francisco
Johnson
Spooner
Westphal
Fox
Himmel

JUN 2 3 1983

If you have any questions concerning this matter, please call Mr. William L. Simkins at extension 3281.


 Jess G. Ross
 2898

Distribution:
 SDL 031

cc:
 NASA Scientific and Technical
 Information Facility
 P.O. Box 8757
 BWI Airport, MD 21240

NASA--NIS-5/Security
 180A/RIAD
 139A/TU&AO

6-15-83
 139A/WLSimkins:elf 06/15/83 (3281)

6-15-83
 139A/JS

4611 2078 BLOC 1194

MAIL STOP 188

31-01 HEADS OF ORGANIZATIONS
 HESS, JANE S.,
 10-1E



0069237

NACA RM No. L8H10

~~RESTRICTED~~

NATIONAL ADVISORY COMMITTEE FOR AERONAUTICS

RESEARCH MEMORANDUM

EFFECT OF AIRFOIL PROFILE OF SYMMETRICAL SECTIONS ON THE
LOW-SPEED STATIC-STABILITY AND YAWING DERIVATIVES OF
45° SWEEPBACK WING MODELS OF ASPECT RATIO 2.61

By William Letko and Byron M. Jaquet

SUMMARY

An investigation was made in the Langley stability tunnel to determine the effect of airfoil profile of symmetrical sections on the static and yawing-stability derivatives of three untapered wings of 45° sweepback. The wings had the following profiles normal to the leading edge: biconvex (12 percent thick), NACA 65₁-012, and NACA 0012. The wings all were of aspect ratio 2.61.

The results of the tests indicate that, of the wings tested, the biconvex wing had the lowest lift-curve slope and the lowest value of maximum lift coefficient.

Of the derivatives resulting from an angle of yaw or a yawing velocity, only the effective dihedral and the rolling moment due to yawing parameter were seriously affected by change in profile shape. The values of both these derivatives were reduced as the sharpness of the wing leading edge increased. It appears that certain qualitative predictions of the trends in these derivatives might be made for plain sweptback wings by using only basic lift and drag data.

For the present low-scale tests the addition of an inboard nose spoiler to the NACA 0012 wing caused a small increase of the maximum lift coefficient, decreased the rearward shift of the aerodynamic center, and caused a small reduction in the maximum value of effective dihedral. The spoiler did not appreciably affect the other stability derivatives of the NACA 0012 wing.

INTRODUCTION

Estimation of the dynamic flight characteristics of aircraft requires a knowledge of the forces and moments resulting from the angular motions of the airplane. The relationship between the forces and moments and the angular motions of the airplane are commonly expressed in nondimensional

~~RESTRICTED~~

terms known as the rotary derivatives. In the past these rotary derivatives have generally been estimated from theory because of the lack of a convenient experimental technique.

The recent application of the rolling-flow and curved-flow principles of the Langley stability tunnel (references 1 and 2), however, has made the determination of the rotary derivatives relatively easy. A systematic research program utilizing these new experimental techniques has been established to determine the effects of various geometric variables on both rotary and static stability characteristics.

The present investigation was made to determine the effects of airfoil profile of symmetrical sections on the low-speed static and yawing characteristics of sweptback wings. One of the wings having a blunt leading edge was tested with and without a nose spoiler extending from the plane of symmetry to the 50-percent semispan of either wing panel to determine whether there might be any advantage in a wing with the section varying from sharp nose at the wing root to round nose at the wing tip. The effect of increased turbulence on the aerodynamic characteristics of the wings in straight flow was investigated. Comparisons of some of the experimental results with theory are also presented.

SYMBOLS

The data are presented in the form of standard NACA coefficients of forces and moments which are referred, in all cases, to the stability axes, with the origin at the quarter-chord point of the mean aerodynamic chord of the models tested. The positive directions of the forces, moments, and angular displacements are shown in figure 1. The coefficients and symbols used herein are defined as follows:

C_L	lift coefficient (L/qS)
C_X	longitudinal-force coefficient (X/qS)
C_D	drag coefficient ($-C_X$ for $\psi = 0^\circ$)
C_Y	lateral-force coefficient (Y/qS)
C_l	rolling-moment coefficient (L'/qSb)
C_m	pitching-moment coefficient ($M/qS\bar{c}$)
C_n	yawing-moment coefficient (N/qSb)
L	lift
X	longitudinal force

Y	lateral force
L'	rolling moment about X-axis
M	pitching moment about Y-axis
N	yawing moment about Z-axis
q	dynamic pressure $\left(\frac{1}{2}\rho V^2\right)$
ρ	mass density of air
V	free-stream velocity
S	wing area
b	span of wing, measured perpendicular to axis of symmetry
c	chord of wing, measured parallel to axis of symmetry
\bar{c}	mean aerodynamic chord $\frac{2}{S} \int_0^{b/2} c^2 dy$
x	distance of quarter-chord point of any chordwise section from leading edge of root section
\bar{x}	distance from leading edge of root chord to quarter chord of mean aerodynamic chord $\frac{2}{S} \int_0^{b/2} cx dy$
A	aspect ratio $\left(\frac{b^2}{S}\right)$
α	angle of attack measured in plane of symmetry
ψ	angle of yaw
Λ	angle of sweepback
$\frac{rb}{2V}$	yawing velocity parameter
r	yawing angular velocity, radians per second

$$C_{L\alpha} = \frac{\partial C_L}{\partial \alpha}$$

$$C_{l\psi} = \frac{\partial C_l}{\partial \psi}$$

$$C_{n\psi} = \frac{\partial C_n}{\partial \psi}$$

$$C_{Y\psi} = \frac{\partial C_Y}{\partial \psi}$$

$$C_{l_r} = \frac{\partial C_l}{\partial \frac{rb}{2V}}$$

$$C_{n_r} = \frac{\partial C_n}{\partial \frac{rb}{2V}}$$

$$C_{Y_r} = \frac{\partial C_Y}{\partial \frac{rb}{2V}}$$

APPARATUS AND TESTS

The present investigation was conducted in the 6- by 6-foot test section of the Langley stability tunnel. The methods and conditions of testing in yawing flow are presented in reference 2.

The models tested consisted of three untapered wings of 45° sweepback and aspect ratio 2.61. The models had the following profiles in planes normal to the leading edge: biconvex (12 percent thick), NACA 65₁-012, and NACA 0012. The plan form of the models and the three profiles are shown in figure 2. Also shown in figure 2 is the semispan leading-edge spoiler which, for some tests, was mounted on the wing with the NACA 0012 section.

All the tests were made with the model mounted rigidly at the quarter-chord point of the mean aerodynamic chord on a single strut support as shown in figure 3. Although the strut projected above the top surface of the wings, it is believed that the effect on the results was negligible.

The forces and moments were measured by means of electrical strain gages contained in the strut. The dynamic pressure at which the tests were made was 24.9 pounds per square foot which corresponds to a Mach number of 0.13. The Reynolds number based on the mean aerodynamic chord of the models was 1,100,000.

The models were tested through an angle-of-attack range from about -2° angle of attack up to and beyond the angle of maximum lift at 0° and $\pm 5^\circ$ angle of yaw in straight flow and at 0° angle of yaw in yawing flow. In the straight-flow tests at 0° angle of yaw, six-component measurements were obtained for each wing. For straight-flow tests at $\pm 5^\circ$ angle of yaw and for yawing-flow tests at values of $rb/2V$ of -0.032 , -0.067 , and -0.088 , only measurements of lateral force, yawing moment, and rolling moment were obtained. Although most of the straight-flow tests were obtained with a turbulence screen in the test section, the data for the wing with the NACA 65₁-012 airfoil section were also obtained without the turbulence screen. The turbulence screen, which consisted of vertical wires uniformly spaced across the tunnel cross section, was placed about 10 feet ahead of the model. As is explained in reference 2, screens of nonuniform spacing are necessary for obtaining yawing flow.

CORRECTIONS

Approximate corrections (similar to those of reference 3), based on unswept-wing theory, for the effects of the jet boundaries have been applied to the angle of attack, the longitudinal-force coefficient, and the rolling-moment coefficient. The lateral-force coefficients have been corrected for the buoyancy effect of the static-pressure gradient associated with curved flow. (See reference 2.) The C_{l_r} tare associated with the induced load resulting from the presence of the strut was obtained for the wing at zero lift coefficient and was applied throughout the lift-coefficient range to the C_{l_r} values.

No other tare corrections have been applied to the data. Corrections for blocking, turbulence, or the effects of static-pressure gradient on the boundary-layer flow have not been applied to these results.

RESULTS AND DISCUSSION

Characteristics in Straight Flow

The lift, longitudinal-force, and pitching-moment characteristics as measured in straight flow are presented in figure 4. The characteristics are similar to results obtained in the Langley 19-foot pressure tunnel and in the Langley full-scale tunnel. From figure 4 and table I, it can be seen that the lowest lift-curve slope at small lift coefficients and the lowest maximum lift coefficient were obtained with the biconvex section. For comparison, table I also contains values of $C_{l_{\alpha}}$ computed by the method given in reference 4 and by Weissinger's method given in reference 5. The highest maximum lift coefficient was obtained with the wing with NACA 0012 airfoil section with inboard nose spoiler. The increase in the maximum lift coefficients obtained with the nose spoiler across the midsemispan also has been indicated from unpublished data of tests on a full-scale triangular-plan-form model. Effectively increasing the sharpness of the leading edge, by changes in airfoil section, caused higher values of the longitudinal-force coefficient at moderate and high lift coefficients. The rather high longitudinal-force coefficients obtained at high lift coefficients for the NACA 65₁-012 wing probably are a result of the low Reynolds number of the present tests.

Increasing the sharpness of the leading edge also reduced the rearward movement of the aerodynamic center with lift coefficient. Of the plain airfoils, the biconvex appears to have the smallest rearward shift of the aerodynamic center. The addition of the nose spoiler to the NACA 0012 wing reduces the rearward shift obtained with the plain NACA 0012 wing.

From figure 5 it can be seen that at low lift coefficients the values of $C_{Y_{\psi}}$ and $C_{n_{\psi}}$ are very small and are little affected by airfoil section. The values of $C_{Y_{\psi}}$ obtained throughout the entire lift-coefficient range are relatively unimportant with regard to airplane stability; however, the $C_{n_{\psi}}$ values are quite important. At moderate lift coefficients the negative values of $C_{n_{\psi}}$ for swept wings may contribute an appreciable amount to stability (of the wings tested, the NACA 0012 wing is the most stable) but at high lift coefficients, the instability (positive $C_{n_{\psi}}$) of the swept wing may offset the stability given by a vertical tail and, thus, may cause the complete airplane to be unstable.

The effects of airfoil sections on $C_{L\psi}$, however, are important. The value of $C_{L\psi}$ is affected both with regard to its maximum value and the lift coefficient at which the curves begin to deviate from their initial linearity. In general, as the airfoil nose shape was made more pointed both the maximum value of $C_{L\psi}$ and the range over which the characteristics were linear decreased.

The addition of the nose spoiler to the NACA 0012 wing had very little effect on $C_{Y\psi}$ and $C_{n\psi}$ but decreased slightly the maximum value of $C_{L\psi}$.

The value of $\frac{C_{L\psi}}{C_L}$ at zero lift coefficient for a 45° sweptback wing of aspect ratio 2.61, given by the theory of reference 4, is 0.0055. This theoretical value is somewhat less than the experimental values with the exception of the value of 0.0050 obtained with the biconvex section. (See table I.)

Most of the data in straight flow were obtained with a turbulence screen about 10 feet ahead of the model to obtain data in straight flow with more nearly the same turbulence condition as obtained in yawing flow. Screens of nonuniform wire spacing are used in yawing flow to obtain proper air-stream curvature. (See reference 2.)

In order to determine the effect of the increased turbulence on the aerodynamic characteristics in straight flow, tests of the NACA 65₁-012 wing were made both with and without a turbulence screen. The effect of turbulence on the lift characteristics and the effective dihedral parameter $C_{L\psi}$ for the NACA 65₁-012 wing can be seen in figure 6. The increase in turbulence caused a slight reduction in lift-curve slope but had no effect on the maximum lift coefficient. The rate of change of $C_{L\psi}$ with lift coefficient and the maximum value of $C_{L\psi}$ were reduced slightly by an increase in turbulence. In general, the turbulence effects seemed to be of negligible importance.

Characteristics in Yawing Flow

Although, in general, the values of C_{Y_r} are lower for the NACA 0012 wing with and without the nose spoiler than the values obtained with the other wings (fig. 7), the values are considered to be of negligible magnitude. The values of C_{n_r} are little affected by airfoil section and the magnitude of the values of C_{n_r} also appear to be negligible. There are,

however, large and important effects of airfoil section on C_{l_r} . The family of curves of C_{l_r} presented in figure 7 very closely resembles the family of C_{l_ψ} curves presented in figure 5. Both the maximum value of C_{l_r} and the lift-coefficient range for linear characteristics are reduced in much the same manner as C_{l_ψ} by effectively sharpening the leading edge by changes in airfoil section. It should be noted that very small positive or even negative values of C_{l_r} may exist at high lift coefficients. Previous tests of unswept wings have shown that the initial positive slope is maintained to the maximum lift coefficient.

A value of the slope $\frac{C_{l_r}}{C_L}$ of 0.277 is predicted by the theory of reference 4 for a 45° sweptback wing of aspect ratio 2.61. This value is much lower than any of the experimented values and compares best with the value of 0.400 obtained experimentally with both the NACA 65₁-012 wing and the biconvex wing. (See table I.)

The addition of the inboard nose spoiler to the NACA 0012 wing caused some changes in the values of C_{Y_r} which are considered to be insignificant. There was very little effect on C_{n_r} ; however, there was a reduction of the maximum value of C_{l_r} and a slight decrease in the lift coefficient at which C_{l_r} began to deviate from linearity.

$$\text{Drag Index, } C_D - \frac{C_L^2}{\pi A}$$

From the similarity noted for the effects of airfoil section on C_{l_ψ} and C_{l_r} it might be expected that some criterion might be selected which would make it possible to make certain qualitative predictions of the trends in stability derivatives by using only basic lift and drag data. A suitable criterion for sweptback wings appears from reference 6 to be the increment of drag not ideally associated with lift or, roughly, $C_D - \frac{C_L^2}{\pi A}$. This increment is plotted for the different wings in figure 8. The lift coefficient at which this increment begins to rise rapidly should indicate the beginning of flow separation from some point on the wing and it is at this lift coefficient that changes would be expected to occur in the stability derivatives. The drag increment (fig. 8) begins to increase rapidly at about 0.6 lift coefficient for the NACA 0012 wing, and from figures 5 and 7 it

can be seen that the values of C_{l_ψ} and C_{l_r} for the NACA 0012 wing began to deviate from their initial linear trends at about 0.6 lift coefficient. For the NACA 65₁-012 wing and for the biconvex wing the increase occurs at about 0.35 and at about 0.25 lift coefficient, respectively, and from figures 5 and 7, it can be seen that changes in the trends of the derivatives C_{l_ψ} and C_{l_r} begin to take place at approximately these lift coefficients for each wing.

This criterion might also be expected to apply to variations of the characteristics with Reynolds number. It has appeared to work out fairly well at least for C_{l_ψ} as indicated by tests made at various Reynolds

numbers in the Langley 19-foot pressure tunnel. From data of this tunnel presented in reference 7, it was found that by increasing the Reynolds number from 1,400,000 to 5,300,000 the deviation of the values of C_{l_ψ}

(for a low-drag airfoil) from the initial linear trends and the increase in the quantity $C_D - \frac{C_L^2}{\pi A}$ were delayed to a lift coefficient almost at the stall.

From the foregoing discussion it appears that the drag increment might be used as a basis for predicting the lift-coefficient range over which the calculated values of the derivatives such as C_{l_r} (usually linear with lift coefficient) might be expected to remain linear. This might be especially true for predicting the Reynolds number effects on the derivatives such as C_{l_r} which normally can be determined in tunnels only at small Reynolds numbers.

It should be noted that the quantity $C_D - \frac{C_L^2}{\pi A}$ might not be as useful in making predictions for other than plain sweptback wings because when devices which delay tip stalling are used, they may cause the quantity $C_D - \frac{C_L^2}{\pi A}$ to show an increase because of separation of flow from inboard parts of the wing which could not greatly affect the rolling- and yawing-moment derivatives.

CONCLUDING REMARKS

The results of low-scale tests made to determine the effect of airfoil profile of symmetrical sections on the low-speed static- and yawing-stability derivatives of untapered 45° sweptback wing models of aspect ratio 2.61 indicate the following:

1. For the wings tested, the biconvex had the lowest lift-curve slope at small lift coefficients and also the lowest maximum lift coefficient.

2. The rate of change of effective dihedral with lift coefficient was the least for the wing with the sharpest leading edge (the biconvex).

3. For the plain airfoils the maximum value of effective dihedral and the range over which the variation of the effective dihedral with lift coefficient was linear decreased as the airfoil nose shape was made more pointed.

4. At zero lift coefficient there was little effect of airfoil section on the rate of change with lift coefficient of rolling moment due to yawing but the maximum value of rolling moment due to yawing and the range for which the variation with lift coefficient remained linear decreased as the airfoil nose shape was made more pointed.

5. It appears that certain qualitative predictions of the trends in the stability derivatives might be made for plain sweptback wings by using only basic lift and drag data.

6. For the present low-scale tests the addition of an inboard nose spoiler to the NACA 0012 wing caused a small increase of the maximum lift coefficient, decreased the rearward shift of the aerodynamic center, and caused a small reduction in the maximum value of effective dihedral over that obtained with the plain NACA 0012 wing. The spoiler did not appreciably affect the other stability derivatives of the NACA 0012 wing.

Langley Aeronautical Laboratory
National Advisory Committee for Aeronautics
Langley Field, Va.

REFERENCES

1. MacLachlan, Robert, and Letko, William: Correlation of Two Experimental Methods of Determining the Rolling Characteristics of Unswept Wings. NACA TN No. 1309, 1947.
2. Bird, John D., Jaquet, Byron M., and Cowan, John W.: Effect of Fuselage and Tail Surfaces on Low-Speed Yawing Characteristics of a Swept-Wing Model as Determined in Curved-Flow Test Section of Langley Stability Tunnel. NACA RM No. L8G13, 1948.
3. Goodman, Alex, and Feigenbaum, David: Preliminary Investigation at Low Speeds of Swept Wings in Yawing Flow. NACA RM No. L7I09, 1947.
4. Toll, Thomas A., and Queijo, M. J.: Approximate Relations and Charts for Low-Speed Stability Derivatives of Swept Wings. NACA TN No. 1581, 1948.
5. Van Dorn, Nicholas H., and DeYoung, John: A Comparison of Three Theoretical Methods of Calculating Span Load Distribution on Swept Wings. NACA TN No. 1476, 1947.
6. Letko, William, and Cowan, John W.: Effect of Taper Ratio on Low-Speed Static and Yawing Stability Derivatives of 45° Sweptback Wings with Aspect Ratio of 2.61. NACA TN No. 1671, 1948.
7. Neely, Robert H., and Conner, D. William: Aerodynamic Characteristics of a 42° Swept-Back Wing with Aspect Ratio 4 and NACA 64₁-112 Airfoil Sections at Reynolds Numbers from 1,700,000 to 9,500,000. NACA RM No. L7D14, 1947.

TABLE I.- COMPARISON OF EXPERIMENTAL AND THEORETICAL VALUES
OF SOME OF THE IMPORTANT AERODYNAMIC PARAMETERS

Airfoil section	C_{L_α} at $C_L = 0$			C_{L_ψ}/C_L at $C_L = 0$		C_{L_r}/C_L at $C_L = 0$	
	Measured	Theory (reference 4)	Theory (reference 5)	Measured	Theory (reference 4)	Measured	Theory (reference 4)
NACA 0012	0.0420	^a 0.0407	^a 0.0395	0.0071	0.0055	0.460	0.277
NACA 65 ₁ -012	.0430	^b .0422	^b .0418	.0071	.0055	.400	.277
Biconvex	.0350	^c .0383	^c .0355	.0050	.0055	.400	.277
NACA 0012 with nose spoiler	.0420	^a .0407	^a .0395	.0074	.0055	.430	.277

^aAssumed section lift-curve slope, 0.099, per degree.

^bAssumed section lift-curve slope, 0.105, per degree.

^cAssumed section lift-curve slope, 0.089, per degree.

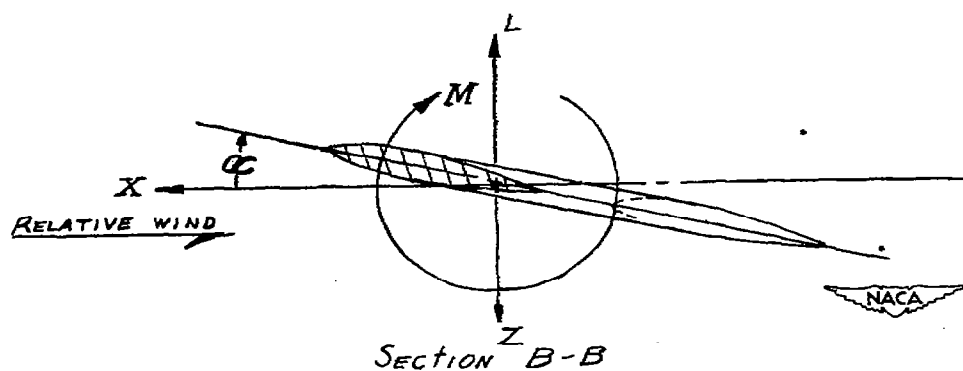
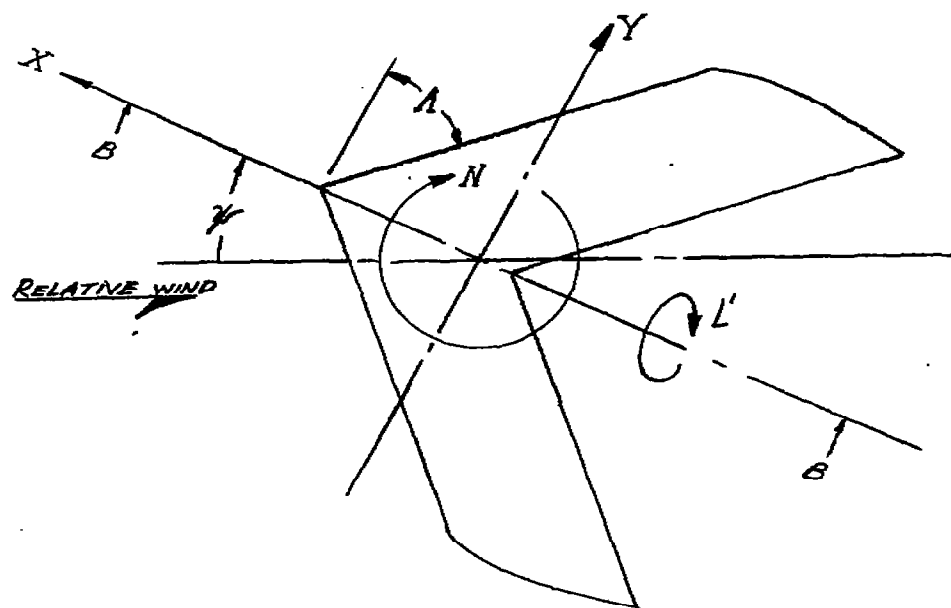


Figure 1.- System of axes used. Positive directions of forces, moments, and angles are indicated.

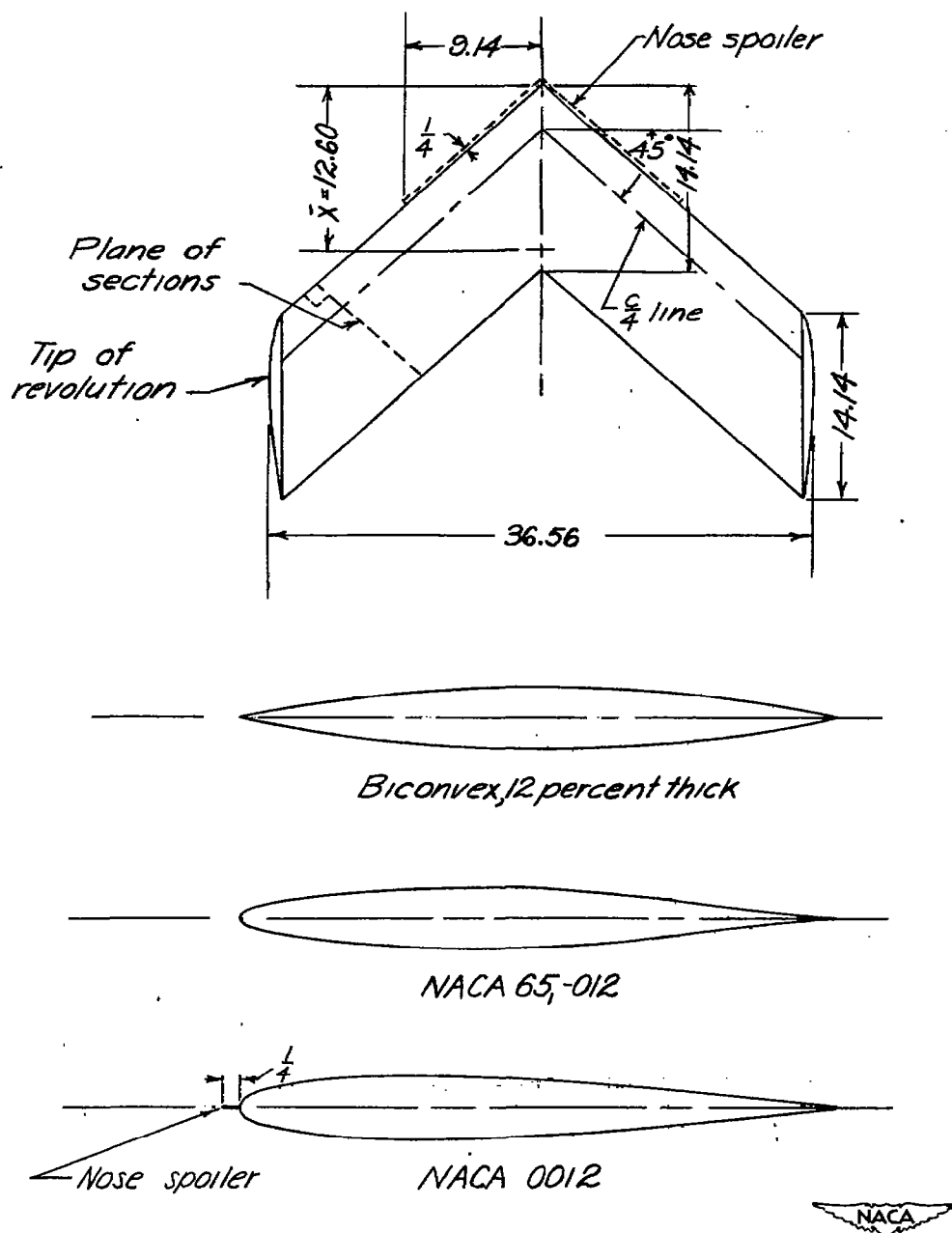


Figure 2.- Sketch of the plan form and airfoil sections of the models investigated. All dimensions are in inches. Wing area equals 3.56 square feet.

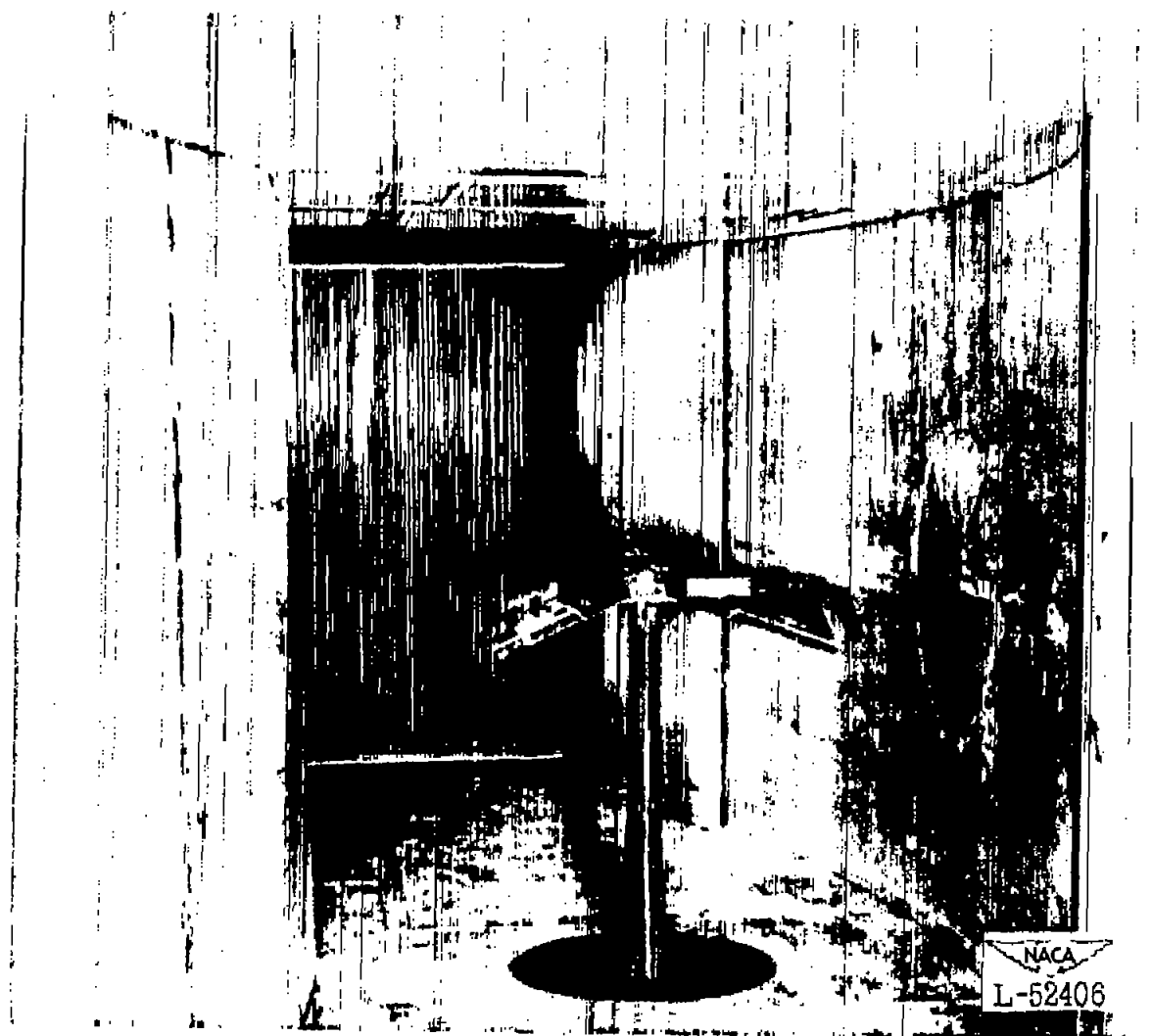


Figure 3.- The 45° sweptback wing mounted in the curved-flow test section of the Langley stability tunnel. NACA 0012 airfoil section.

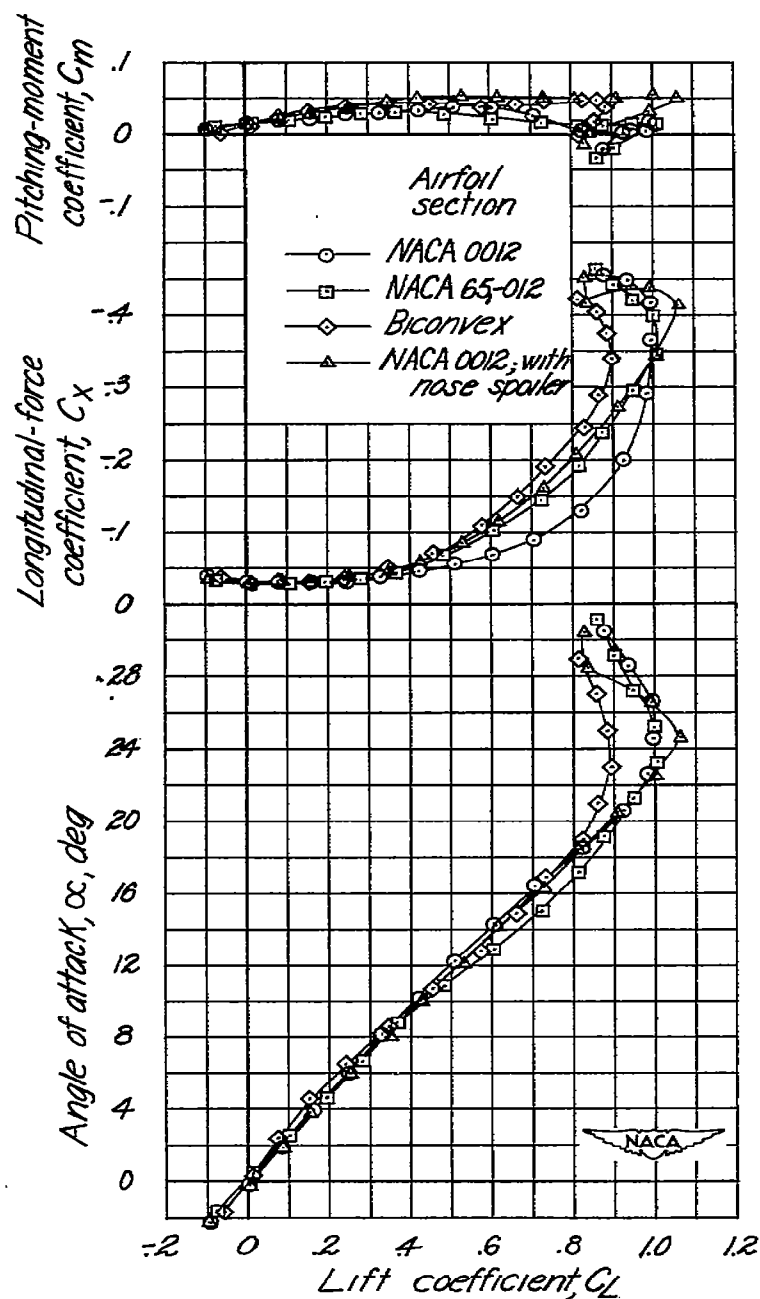


Figure 4.- Variation of pitching-moment coefficient, longitudinal-force coefficient, and angle of attack with lift coefficient for the wings tested. Uniform screen in tunnel. $R = 1.1 \times 10^6$.

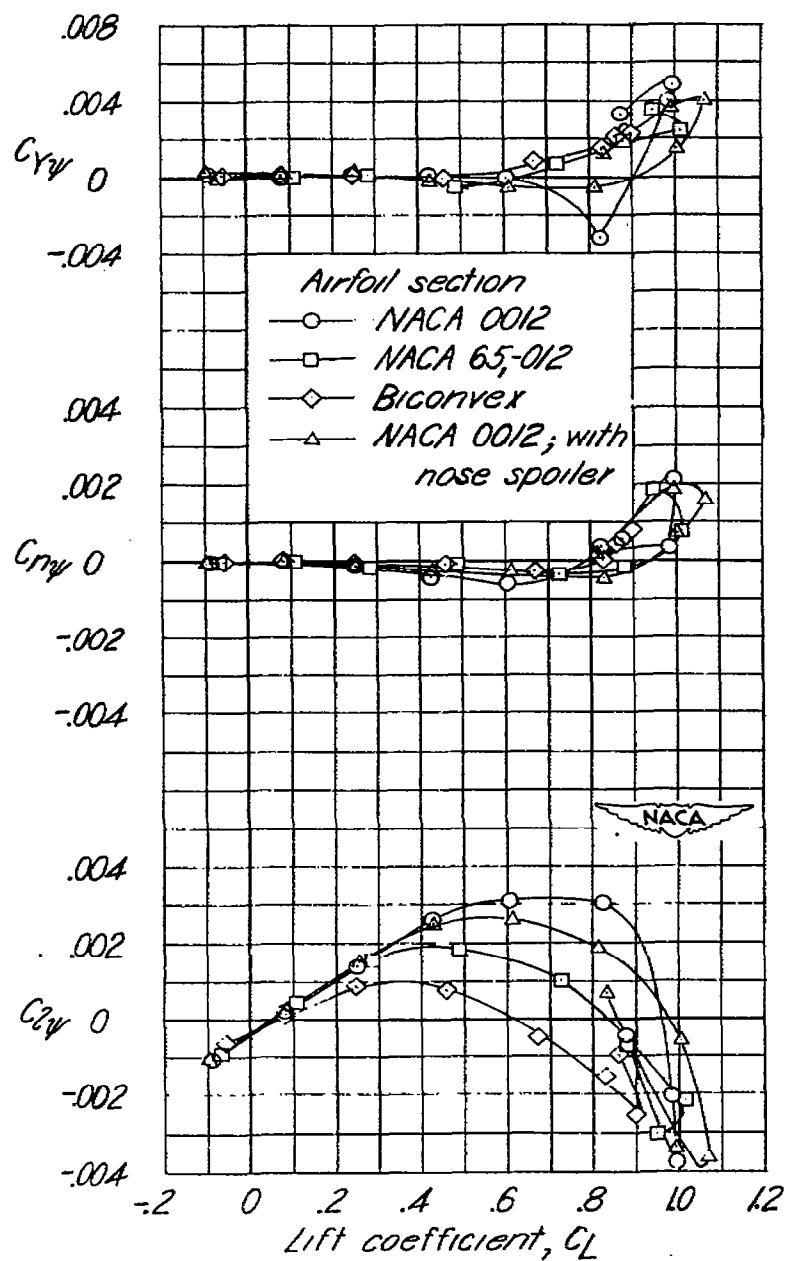


Figure 5.-Variation of $C_{Y\psi}$, $C_{N\psi}$, and $C_{Z\psi}$ with lift coefficient for the wings tested. Uniform screen in tunnel. $R = 1.1 \times 10^6$.

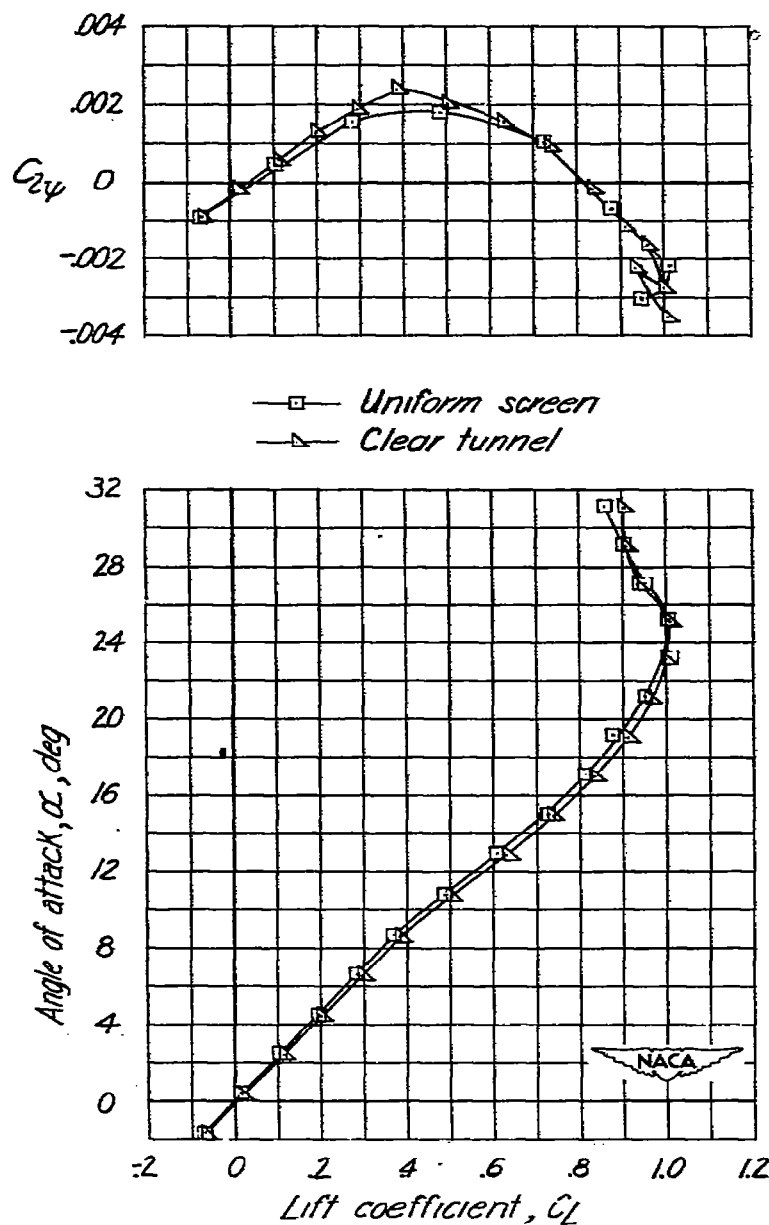


Figure 6.- Variation of the angle of attack and $C_{2\psi}$ with lift coefficient for the NACA 65,-012 wing with and without a uniform screen in the tunnel. $R=1.1 \times 10^6$.

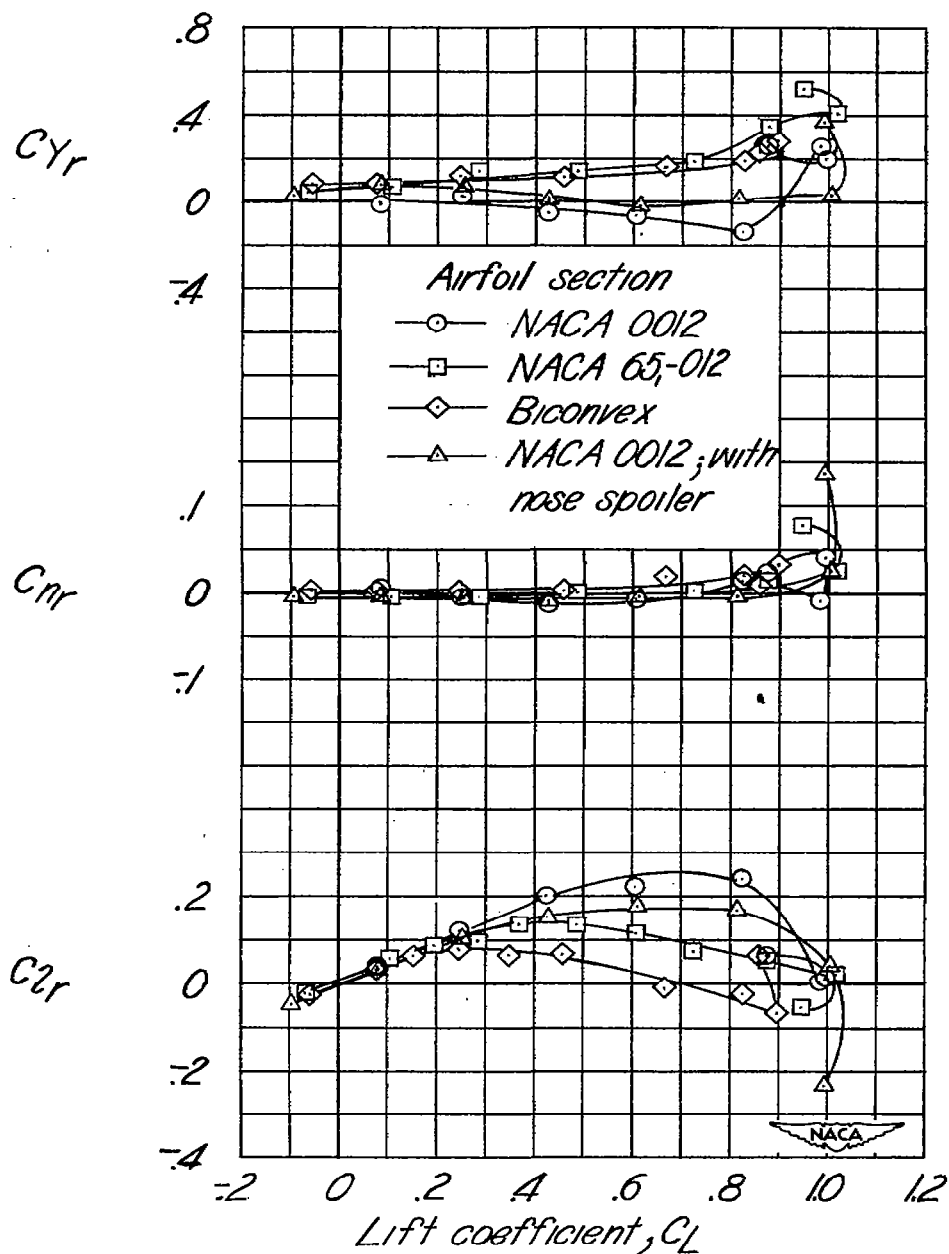


Figure 7.—Variation of C_{Y_r} , C_{N_r} , and C_{L_r} with lift coefficient for the wings tested. $\psi = 0$; $R = 11 \times 10^6$. Nonuniform screens in tunnel.

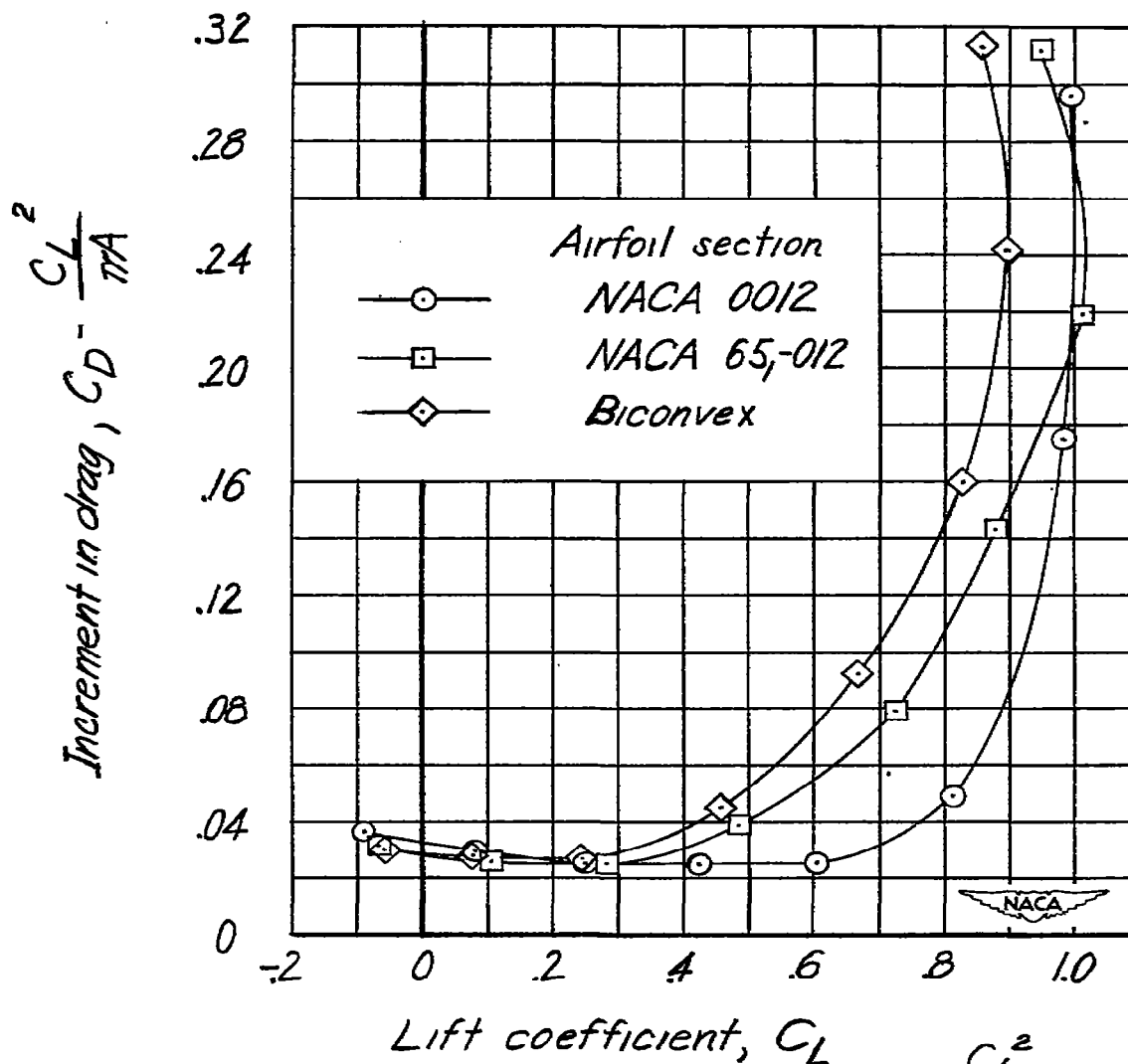


Figure 8 - Variation of the increment in drag $C_D - \frac{C_L^2}{\pi A}$ with lift coefficient for the wings tested. Uniform screen in tunnel.